

Design and Experimental Investigation of Pneumatic Movement Mechanism Supported by Mechanic Cam and Crank Shaft

Salih KORUCU¹, Gürcan SAMTAŞ², Gürkan SOY³,

¹Gazi University, Faculty of Technology, Department of Manufacturing Engineering, Beşevler, Ankara, Türkiye

²Düzce University Engineering Faculty, Department of Mechatronics, Beci, Düzce, Türkiye

³Uzer Machine and Molding Industry Incorporated Company, Kocaeli, Türkiye

Abstract–The pressurized air is applied to many sectors required purity and velocity. One of these sectors is to use of air as impulsive force in the moving mechanisms. In this study, the movement mechanism prototype worked with compressed air was designed and produced for light vehicle engine as motorbike and ATV (All-Terrain Vehicle). In developed mechanisms, pneumatic artificial muscles were used for a given movement of crankshaft. A cam system was also designed for synchronization pneumatic muscles. In this way, these muscles transmit the synchronous movement to crankshaft. At the end of the study, the developed mechanism was mounted on an ATV vehicle (110 cc/ Cubic Centimeter, engine displacement capacity) and its performance was tested using the four different weights (50, 75, 100 and 150 kg), three different pressures (4, 5 and 6 bar) and two different hoses (Ø 6 and Ø 8 mm). By considering experimental results and design criteria, power of the movement mechanism was obtained as 886 Watt. With this study, minimization of energy consumption for movement of passenger cars, and using clean and cheap energy as ATV which can be alternative for single or two passenger vehicles.

Keywords – Pneumatic artificial muscle, ATV air vehicle, compressed air, pneumatic mechanism.

1. Introduction

Today, bicycles and motorcycles are light vehicles used for a short distance. Oil is the main fuel source of transportation vehicles, and it is gradually running out, it is expensive and it is especially harmful to the environment. Actuation principle and transmission of the compressed air used in vehicles is very similar to a steam engine. Compressed and expanding air instead of the fuel mixture and the combustion process is used to move the piston into the motor [1]. In this system, high-pressure air pushes the piston, and movement occurs [2]. This motion can produce power that can be used as an alternative to today's internal combustion petroleum-

derived fuel vehicles. Technical difficulties in the production of petroleum promote air energy using in industry [1]. When compared to these two types of vehicles, the air powered vehicles have several advantages. For example, it can be used in the environment friendly energy source which does not require in any way of hydrocarbon fuel [3]. It is found in free form in nature and is abundant, affordable, portable and does not pollute air we breathe [1], [4] and [5]. Therefore, air vehicles do not need a cooling system and spark plugs, and the compressed air has lowered to about 20% of the production costs of vehicles. The design of its engine is simple and strong. Operation and maintenance costs are low and easy. [1] and [5]. It produces high torque at minimum volume. While the air is compressing at a reasonable speed, it heats. After this compression, this liberated heat can be used in heating systems or the Stirling engine [1]. Exhaust gasses released from the engine are slightly less than the atmospheric temperature [5]. In addition, air vehicles contribute greatly to the reduction of environmental pollution formed with vehicles powered by petroleum [1],[3],[5] and [6].

Koca and Sağır [7], the tracked pneumatic motor was designed and produced without crankshaft, camshaft and valves. The four studies were conducted with four pallets located on the eccentric rotor engine in each cycle. Pneumatic motor directly converted compressed air power to rotational movement. Only a very small amount of oil and fresh air from the exhaust were discarded. The developed prototype working pressure was 8,9 and 10 bar, and its highest rotation was 1300 rev/min as unloaded. Manish et al. [3] investigated to design and production of a single cylinder engine worked with compressed air. The main purpose of this study was to run motorcycle and bicycle engines with compressed air making a few modifications. Mohammad [8], making changes on the single-cylinder engine, evaluated it in terms of brake power,

indicated power, mechanical efficiency and volumetric efficiency. He examined the MDI air-powered engine of the French engine manufacturer. This engine had air motor with two cylinders, and it was operated as internal combustion engine. In this study, the energy required to move the vehicle was provided by the high-pressure carbon fiber air tank placed under the vehicle. This vehicle speed was 110 km/h and it has a range of 200 km [6]. Yadav and Singh produced an air engine prototype to be operated with compressed air in the single-cylinder low-speed air motor. In this work, compressed air used to increase the starting torque [4]. In the other study of motor powered by compressed air, Patel et al. investigated capacity of air engine. In their study, they observed the engine worked smooth, knocks and stated that the occurred minimum wear on the engine and its components [5].

The air vehicles, it usually has a tank compressed air, and it is mechanic systems that produced work operating with air motors. Although there is not sufficient literature published in this area, most of studies are on existing engine components used to be converted to the system operating with air. Therefore, the different solutions, which will convert mechanic motion, to circular motion are required. In this study, a movement mechanism working with compressed air was developed for light vehicle engine using the pneumatic artificial muscle (PAM) and other pneumatic circuit elements. In addition, suitable with movement system mechanical cam and crankshaft was designed and developed for the movement of the mechanism. This developed movement mechanism was mounted to ATV vehicle

having a capacity of 110 cc, and it was tested with different pressures and different hose diameters. The results of the experiments were interpreted with graphics and tables, and these results were evaluated.

2. Design of a pneumatic mechanism

Pneumatic drives, along with hydraulic and electric ones are one of the basic types of drives used in mechanization and automation of manufacturing processes. Increased speeds result in higher performance of pneumatic drives. Their applications in the industrial processes require high speeds of actuators or high kinetic energies [9]. The motion of the pneumatic movement mechanism consisted of artificial muscles conducting with pneumatic stimulation moved transmitting to crankshaft. In the mechanism for this motion, a cam system was designed to synchronize pneumatic valves and crankshaft. In addition, this mechanism included pneumatic muscle, crank shaft, rolling bearings, chains, friction gear meshes, sheet metal, cam system and valves (Figure 1).

Pneumatic muscles and valves were provided by Festo Company. The designed the mechanism, pneumatically-driven muscles convulsively were contracted by compressed air, and these contracted muscles are trying to rotate by pulling the crankshaft. Thus, friction gear meshes connected to the crankshaft and chains are driven by muscles. Rotary motion is transmitted to wheels. System activating circuit elements are shown in Table 1 and circuit schematic is shown in Figure 2.

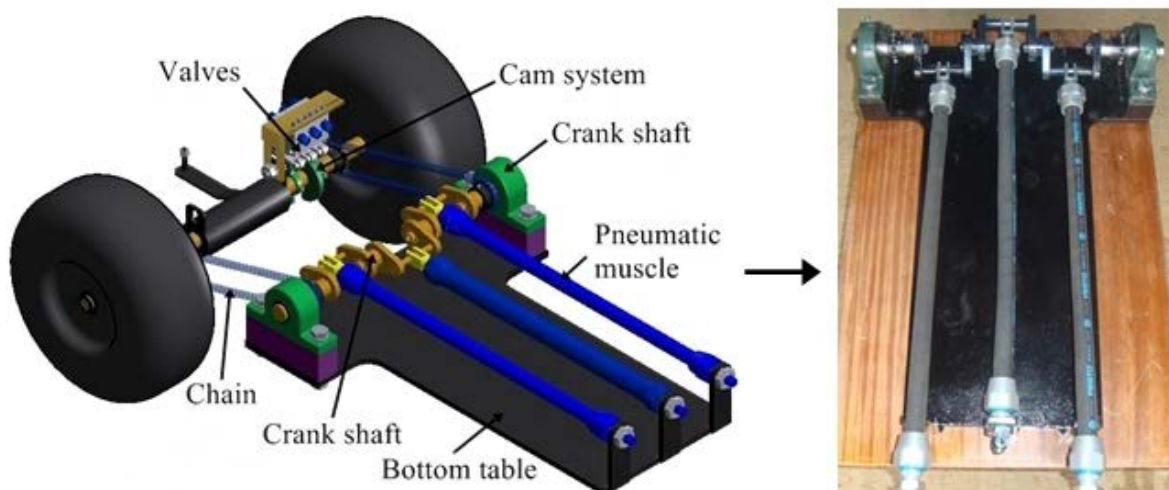
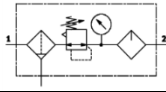
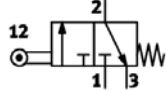
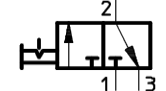
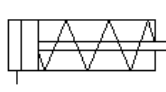


Figure 1. Fabricated of movement mechanism

Table 1. Pneumatic circuit components used in mechanism

| Symbol No | Circuit Symbol | Type | Description |
|-----------|---|---------------------------|---|
| 1 |  | FESTO-FRC-1/4-D-MIDI | Filter, regulator and lubricator functions in a single unit, flow rate 80...8700 l/min. |
| 2 |  | FESTO-VMEM-DT-M32C-M | 3/2-way roller level valve, mono-stable, normally closed, mechanical spring return, Flow rate 80...500 l/min. |
| 3 |  | FESTO-HE-D-MINI | 3/2-way manual shut-off valve. Flow rate 1000...6500 l/min. |
| 4 |  | FESTO-MAS-20-200N-AA-MC-0 | Fluidic Muscle, diameter size 20 mm, nominal length 500 mm, maximum additional load 80 kg. |

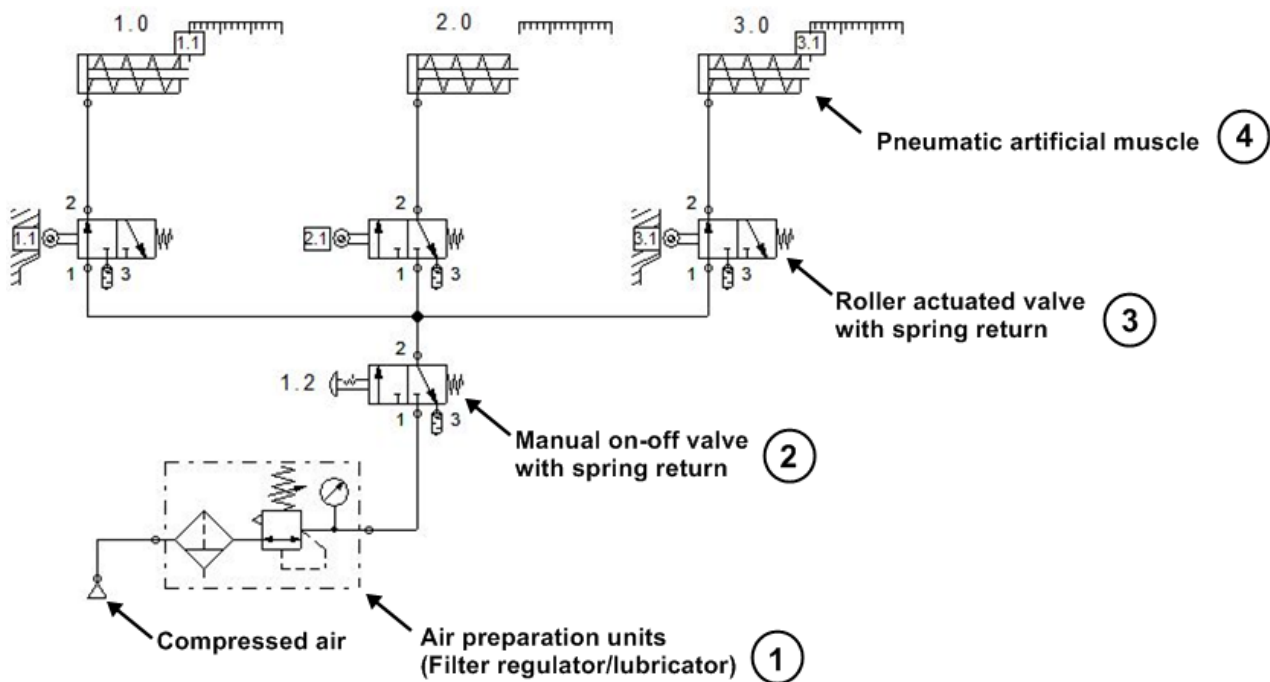


Figure 2. Pneumatic circuit schemas for mechanism

Pneumatic muscles in the mechanism are controlled by three roller valves located in Figure 2. The pressurized air, which is stored in the air tank, is regulated by air preparation unit according to working pressure (4.5 and 6 bar). The prepared air is reached to switch valve by means of an on-off valve. When the on-off valve is opened, signals obtained from the switched on valves according to the position of cams located on the shaft of the wheel are transmitted air to the mechanic system. Thus, the pneumatic muscles are actuated, and this system starts to move. In here, muscle sync and efficient

usage of pressurized air are also an important criterion. In this study, the semi-circle cams were designed to provide muscles sync and without using additional components to hold minimum air consumption level (Figure 3). When the wheels turn, they will turn to these mechanic cams and the turned cams pressed on the valve rollers. The sync air obtained from roller level valves is contracted to pneumatic muscles, and then circular movement is created.

2.1. Cam system and crankshaft design

Cam mechanisms convert a regular driving movement into a movement obtained by an intended cycle function [10]. In this study, cams are in semi-circle shape. They have 125 mm peripheral length

and 10 mm thickness. They were fixed on the movement mechanism to steer the air gone to pneumatic muscles. The used crankshaft was rotated by cams a half tour in order to let a muscle perform complete action. To provide this motion, cams were manufactured to 125 mm length (Figure 3).

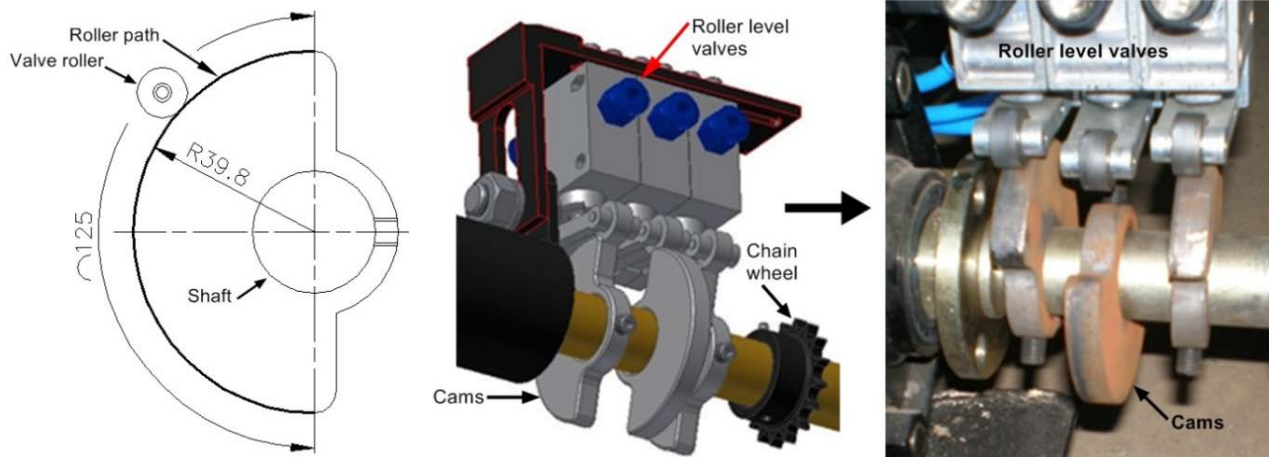


Figure 3. Manufacturing of mechanic cam

As shown in Figure 3, Size of cams is same and fixed on the shaft with respect to position of crankshaft. Crank shafts used in internal combustion engines are mostly eccentric shafts, and they convert rectilinear motion to rotational motion [11]. In the movement mechanism, this motion was provided by artificial muscles. Transformation between two axes was supplied via of chain gears on crankshaft and wheel

shaft. The produced crankshaft was made of the C45 tempered steel, and it was used in the production of vehicle, machine, engine and apparatus. Stages of production of the crank shaft are shown in Figure 4. Crank shaft in movement mechanism is designed and manufactured as 250 mm radius (Figure 4).

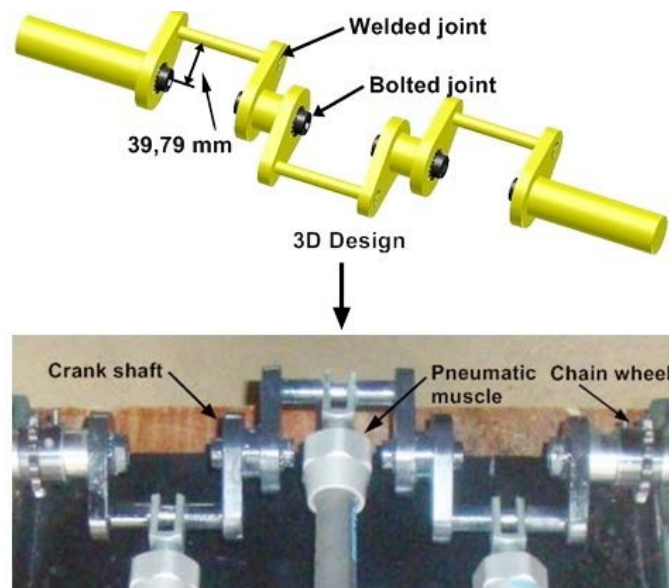


Figure 4. Stages of crankshaft

The crankshaft motion is transmitted to wheels via of chain gears as shown in Figure 4. Control parameters were selected to calculate under maximum conditions for the produced crank shaft. These conditions were used in the conducted experiments at the end of the study. Shafts are exposed to constantly changing turning and bending moment [12]. By considering maximum force

produced by this mechanism, pneumatic muscles under condition of 6 bar pressure and 4500 N force (1500x3) were selected according to manufacturer catalog. In addition, torsional moment, bending moment and shear stress calculations for crankshaft and chain gears were calculated to control design criteria.

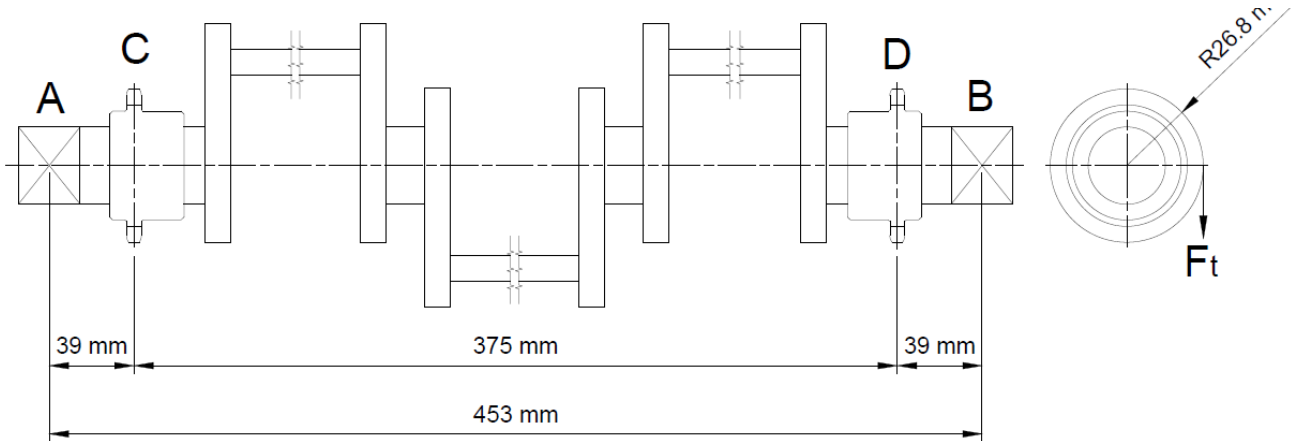


Figure 5. Motion assembly crankshaft and chain gear

Sizes of crankshaft and chain gear used in motion assembly are given in Figure 5. Where A left bearing, B is right bearing, C and D chain gears, distance between chain gear and bearing is 39 mm, distance between chain gears is 375 mm, distance between bearings is 453 mm, radius of C and D chain gears is 26.8 mm, and F_t is tangential force. Motion power is essential to control crank shaft and chain gears. It was calculated as 866 Watt using maximum muscular force (4158 N) and maximum conditions according to experiment results (52 m track / 122 sec time, 108108 Nm work). With these conditions; torsional moment, bending moment and shear stress for the crankshaft were calculated using following formulas [13]. In Eq.1, formula of bending moment produced by shaft at maximum power is shown.

$$T = \frac{60P}{2\pi N} \quad (1)$$

Where, T is the transmitted torque (Nmm), P is used for motor power (Watt), and N is revolution speed (rev/min). In this condition, turning moment transmitted by the shaft was calculated as 235018.799 Nmm. This formula below is used for tangential forces at points C (F_{tC}) and D (F_{tD}) [13];

$$F_{tC} = F_{tD} = T / e \quad (2)$$

Tangential forces were calculated as 8769.358 N according to In Eq.3. Moreover, 5 N of chain gear weight was added to these forces for downward loads at points C and D. Accordingly, tangential forces at points C and D (F_{tC} , F_{tD}), were calculated as 8774.358 N. In this condition, the total force at A and B bearings obtained these two forces was calculated as 17548.716 N. Thus, each bending moment at points C and D were calculated as 3422199.969 N, by using 39mm distance. The bending moment and shear stress of the shaft can be calculated these following equations and making use of the above calculations [13].

$$T_e = \sqrt{(K_m M)^2 + (K_t T)^2} \quad (3)$$

$$\tau = \frac{T_e 10^3 16}{\pi \cdot d^3} \quad (4)$$

In Eq.4 and Eq.5, K_m is bending fatigue and K_T is shear fatigue and combined knock factor, M maximum bending moment, and T is turning the moment transmitted by the shaft and τ is shearing strength of the shaft while turning. Shearing strength of the crankshaft was calculated as 117.459 N/ mm² using these parameters. Another parameter for safety control of the shaft is working stress. The working stress can be able to calculate with primarily bending moment on the shaft (Eq.5).

$$M_e = \frac{1}{2} \left[K_m M + \sqrt{(K_m M)^2 + ((K_i T)^2)} \right] \quad (5)$$

Working stress from bending moment formula is calculated with this following equation [13];

$$\sigma_b = \frac{M_e 10^3 32}{\pi d^3} \quad (6)$$

In the result of controlling crank shaft and chain gears, shear was found 117,458 N/mm² and working stress as 214,281 N/mm². Ultimate strength of C45 tempered steel was $\sigma_k = 700$ N/mm², and its viscosity was $\sigma_{ak} = 490$ N/mm², bending resistance was $\sigma_e = 370$ N/mm² and shearing strength was $\tau = 260$ N/mm². Thus, it was shown that a crank shaft and chain gear can be operated under maximum conditions.

2.2. Selection of PAM and derivative of mathematical model

Pneumatic artificial muscle is a pneumatic actuator which converting pneumatic force into pulling forces [14]. PAMs have more advantages when they are compared to other cylinders in terms

of the high strength, soft and flexible structure, minimum compressed air consumption, and low cost. Therefore, they are used widely in industry, and mechanical behaviors should be completely understood to obtain optimum usage and design conditions in the industry [14], [15] and [16]. Pneumatic muscle can be made of different structure and material depending on Producer Company. On the other hand, they perform different mechanical behavior depending on intended use for acting like a spring, and for this reason different mathematical models can be described on PAMs applications [17], [18] and [19]. In this study, turning radius of a crank shaft is 250 mm, and maximum pressure value is selected as 6 bars. PAMs stroke as 125 mm were chosen from the catalog of the producer company by considering these parameters. PAMs can be extended up to a maximum of 25% of muscle size length. In this study, 500 mm in length PAMs were selected as four times the size of the stroke. Maximum force produced with PAMs during operation was calculated theoretically by considering literature studies, and the obtained value was compared with catalog values. PAMs are force transmitting components. Their modeling as mathematical is difficult, and they have a nonlinear structure [14], [20], [21] and [22].

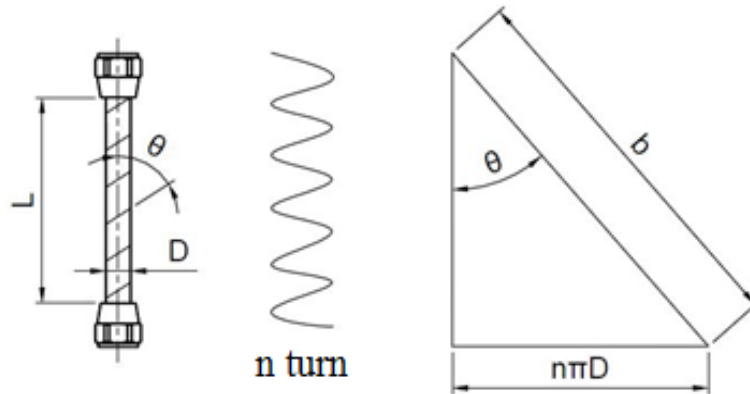


Figure 6. Relation between pneumatic muscle and its radius [23,24]

The required parameters for mathematically modeling of PAM are shown in Figure 6. Where L is natural size of the muscle (mm), similarly D is the radius of the muscle (mm), θ is angle between muscle convolutions and centerline along L. Convolution, which similar a screw cog, occur on muscles depending on the material type used in the production of the muscle [23] and [24]. Number of these convolutions is represented with n. When a right triangle formed by one convolution is examined, convolution length is described as hypotenuse of the triangle (b, mm). Therefore, the

conservation of energy law can be used in order to obtain the force produced by the muscle a function of contraction and pressure according to muscle [25-29]. In this study, MAS-20-500N-AA-MC-O coded product produced by FESTO Company was used, and it was structurally similar to Mckibben kind muscle type:

$$dW_{in} = \int_{s_i} (P - P_0) \times dl_i \times ds_i \quad (7)$$

Here, P is absolute, P_0 is the atmosphere and effective pressure, and s_i is total inner surface. When

exterior structure of the muscle is examined, the force, it produced is shown as in equation below [23],[24] and[29]:

$$dW_{out} = -Fdl \quad (8)$$

According to virtual work principle [23], [24], [29] and [30] ;

$$dW_{in} = dW_{out} \quad (9)$$

$$- Fdl = P' dV \quad (10)$$

$$F = -P' dV / dl \quad (11)$$

While dV / dl rate is obtained, the muscle is considered as an ideal cylinder having no thickness and elongation of ropes is very low. Diameter of muscle for this condition [23],[24] and[29]:

$$D = \frac{b \sin \theta}{n\pi} \quad (12)$$

The following equation is used for explaining muscle volume (V) [23], [24] and [29]:

$$V = \left(\frac{b^2}{4\pi n^2} \right) \sin^2 \theta \cos \theta \quad (13)$$

When inner of the muscle is swelled with compressed air, it inflates and so shrinks. Volume calculation explained in Eq. 14 is the calculated value without considering the thickness and its unpressurised position. When Eq. 6, is replaced in Eq. 4, F force can be written as a function of P' and θ' [23]:

$$F = \frac{P'b^2(3\cos^2 \theta - 1)}{4\pi.n^2} \quad (14)$$

Pneumatic artificial muscle performs similar behavior to single acting cylinder under pressure, but it shrinks instead of elongation. Calculated F force will be obtained at negative direction because of contraction event occurs in negative direction. Convolution length was found (b, mm) 1270.421 mm

by using Eq.13 and cylinder volume (V , mm^3), was found 136505.235 mm^3 . Three different values of pressure as 4, 5 and 6 bars were used in theory calculation of muscular forces. F forces were obtained as -924 N (4 bars), -1155 N (5 bars) and -1386 N (6 bars) respectively. In movement mechanism, three PAMs were used. Direction of movement of all three muscles was same, and crank shaft, which provides movement, was operated through. Maximum pressure used as 6 bars in experiments. The calculated force with this pressure value was 1386 N (for three muscles 4158 N). When producer PAMs catalog is examined, the force under maximum 6 bars pressure for one muscle is defined as 1500 N. McKibben types of muscles are generally made of fiberglass, rubber and nylon fiber material. But Producer Company of the selected muscle, membrane structure of this product produces from materials of chloroprene and aramid. Thus, there is a difference between calculated force and catalog values. In this study, Eq.12, Eq.13, and Eq.14 are suggested for mathematical modeling of MAS-20-500N-AA-MC-O coded product.

3. Experimental results and discussions

3.1. Experimental design

In order to test the developed mechanism, a Mondial at 110 cc motor power small ATV (All-Terrain Vehicle) was used. This ATV's engine was disassembled, and its framework was used for applications. Frame work of vehicle body was elongated with 320 mm iron bars by considering sizes of pneumatic artificial muscles (Figure 7).

Different pressure, nose diameter, and weights were used in experiments of movement mechanism to test its performance. In these experiments, average human weight was considered as 75-85 kg, and maximum 150 kg weight was used. Three 50 kg circular weights and a 25 kg circular weight were prepared for tests. One piece 50 kg weight was used for 50 kg test, one piece 50 kg and one piece 25 kg weights for 75 kg test, two pieces of 50 kg weights for 100 kg test, and three pieces of 50 kg weights for 150 kg tests (Figure 8).

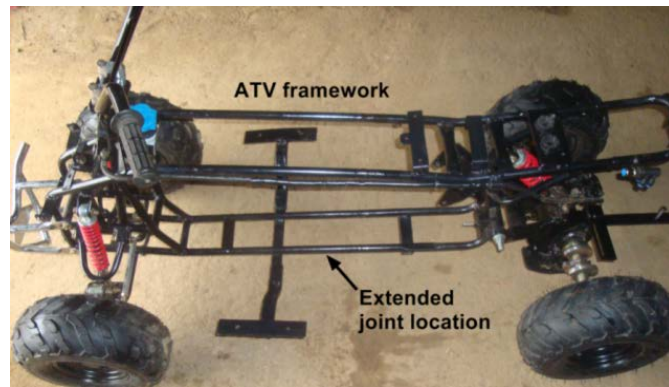


Figure 7. The extended ATV framework



Figure 8. The used weights and preparation of mechanism for test experiments

Apart from the weights used in movement experiments, 6 and 8mm diameter air hoses, 4, 5 and 6 bars pressure values were used by complying catalog values. Two pieces 20 liters of air tank of Festo Company and a Festo FRC-1/4-D-Midi air service unit was used for pressurized air needs of mechanism. Air tanks were pressurized with 10 bar pressure before each experiment, using oxygen gas in order to fill and pressurize the tanks quickly.

3.2. Evaluation of test results

Experiments were performed in consideration of distance (meter), time (second), and speed (m/sec) of the vehicle parameters. System pressure in the air tank pressurized 10 bars for each experiment was lowered to pressure values used in experiments, by using pressure regulating valve. The values obtained from experiments conducted with 8 mm hose are shown in Table 2.

Table 2. Experimental results for 8 mm hose

| Pressure | 4 Bar | | | 5 Bar | | | 6 Bar | | |
|----------|--------------|----------|-----------|---------|----------|-----------|---------|----------|-----------|
| | Distance (m) | Time (s) | Speed m/s | Way (m) | Time (s) | Speed m/s | Way (m) | Time (s) | Speed m/s |
| 50 kg | 50 | 112 | 0.45 | 44 | 90 | 0.49 | 44 | 90 | 0.49 |
| 75 kg | 48 | 117 | 0.41 | 42 | 96 | 0.44 | 42 | 91 | 0.46 |
| 100 kg | 48 | 128 | 0.38 | 42 | 100 | 0.42 | 40 | 91 | 0.44 |
| 150 kg | 38 | 106 | 0.35 | 34 | 100 | 0.34 | 36 | 85 | 0.42 |

Distances that the vehicle taken, time and speed in experiments performed with 8 mm hose, are shown in Table 2. When pressure increases, distances decrease accordingly. This condition reduces the air consumption in tank at existing capacity, and so the vehicle can get far in short distances. On the other hand, increase of the weights reduced the distance. As Ø 8 mm hose used in this experiment was bigger

than Ø 6 mm hose in respect of sectional area of hose, it was seen that rapid pressure decrease arisen and in this condition vehicle moved forward shorter distances (Figure 9 and Figure 10). The vehicle gets far maximum 50 m at 0,45 m/sec, and it completed this track at 112 seconds.

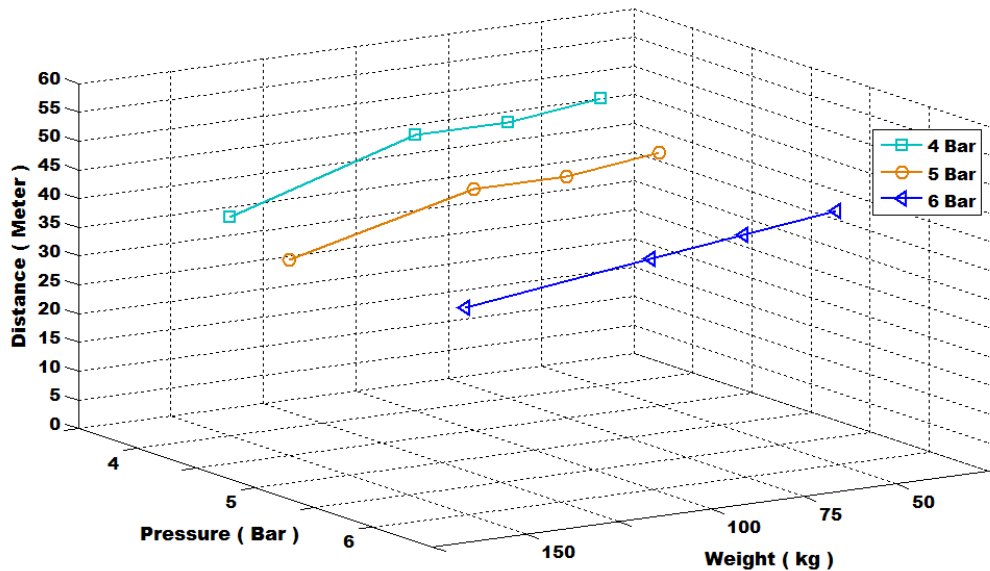


Figure 9. Distance graph of 8 mm hose

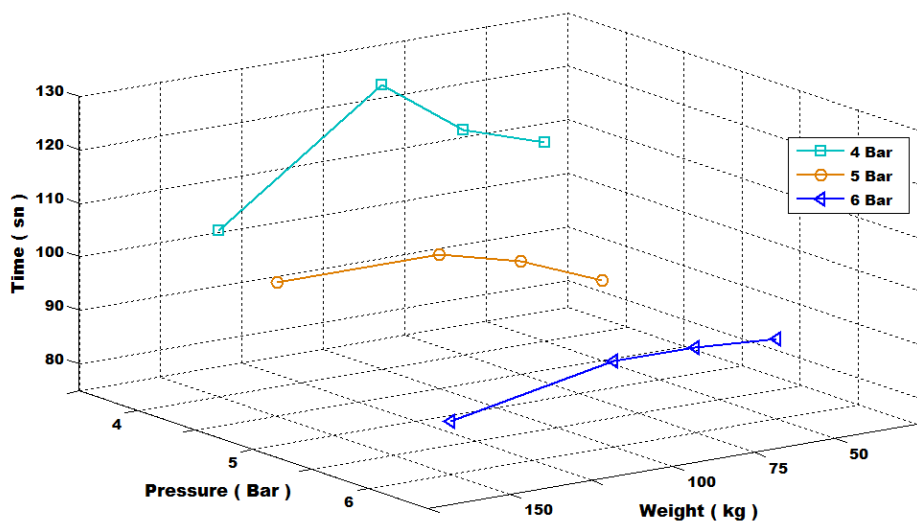


Figure 10. Time graph of 8 mm hose

Distances covered with 8 mm hose with three different pressure and weights are shown in Figure 9. The longest distance is obtained with 4, 5 and 6 bars pressures respectively. As the load increased distances reduced, and the longest distances are obtained with 50 kg weight. The vehicle did not show rapid reaction with 100 kg weight. Distance covered of vehicle reduces under the condition that in 150 kg loading.

Taken of durations of the vehicle are given using same weights and pressures in Figure10. It is shown that the vehicle reaches a longer duration under 4 bars pressure, and this condition can be monitored (Figure 10). Increase of time it moves opposite increasing the load weight reduces distances covered. The raised time reduced the movement distance, and this also reduced the speed. Moreover, pressure increase in a constant pipeline was enhanced force

and speed of the vehicle. Since the high force consumed the existing pressure quickly, it caused 10 bars pressurized oil tank to run out of in a shorter time. As pressure increase in the same volume means that more air is forced into this volume, air consumption will also enhance with pressure

increase. Same experiments were conducted with 6 mm hose, in order to evaluate this condition better (Figure 11 and Figure 12).

Table 3. Experimental results for 6 mm hose

| Pressure | 4 Bar | | | 5 Bar | | | 6 Bar | | |
|----------|--------------|----------|-----------|---------|----------|-----------|---------|----------|-----------|
| | Distance (m) | Time (s) | Speed m/s | Way (m) | Time (s) | Speed m/s | Way (m) | Time (s) | Speed m/s |
| 50 kg | 64 | 143 | 0.45 | 52 | 121 | 0.43 | 52 | 120 | 0.43 |
| 75 kg | 56 | 120 | 0.47 | 52 | 114 | 0.46 | 50 | 111 | 0.45 |
| 100 kg | 58 | 135 | 0.43 | 52 | 119 | 0.44 | 50 | 114 | 0.44 |
| 150 kg | 52 | 122 | 0.42 | 46 | 124 | 0.37 | 42 | 109 | 0.35 |

The distances covered of the vehicle, times and speeds in these experiments performed with 6 mm hose are shown in Table 3. In Table 3, the highest distance was achieved under maximum 4 bars pressure, 50 kg weight with 6 mm hose, average 0.45 m/sec speed and in 143 seconds (Figure 11 and Figure 12). It was provided a longer distance, because of low pressure reduced the air consumption, and used small diameter of hose.

Similarly, it is shown in Table 3 that distances decrease as pressure increases, and under the 5 and 6 bars pressure these distances are also equal. In this conducted experiment with 6 mm hose, a considerable pressure difference was not seen for these two pressures, at 50 kg weight. The important factor here is that hose diameter and length should be kept as low as possible. This condition increased the distance covered of vehicle, and it prevented abrupt pressure drop in existing tank.

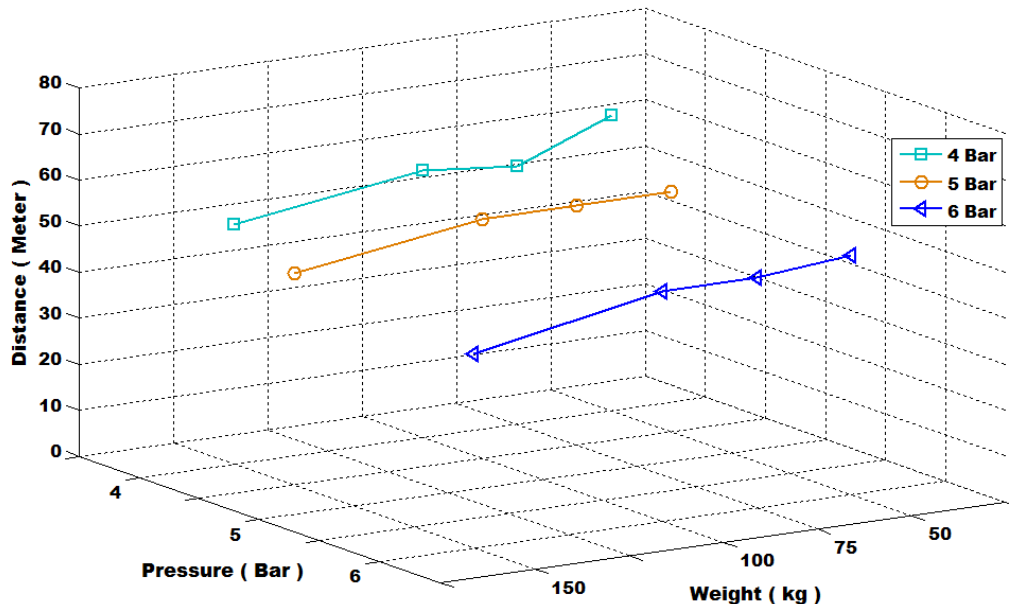


Figure 11. Distances covered against different weights with 6 mm hose

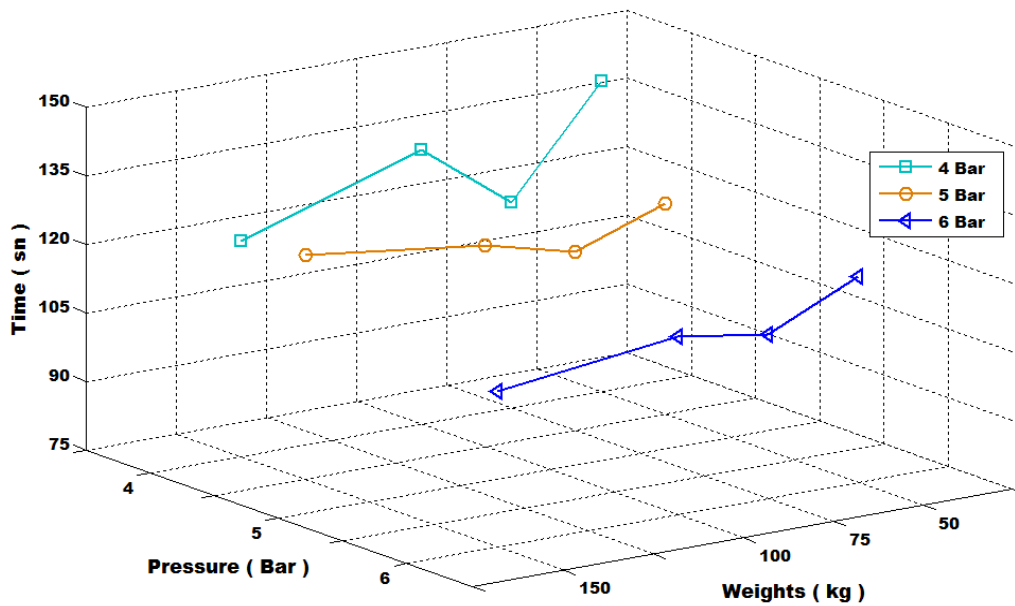


Figure 12. The taken time against different weights with 6 mm hose

In Figure 11, the distances covered against different weights using 6 mm hose in the mechanism are shown. Pressure increase by decrease of hose diameter, and decrease of air consumption caused to be obtained longer distances. In this experiment, the longest distances were obtained with 4 bars pressure. In all pressure experiments, the highest level was reached with 50kg weights, and as the weights rose the distances covered decreased. A graph does not show any immediate change. It shows sudden drop for 150 kg weight. These results are similar to 8 mm hose diameter experiments, and same similarities also obtained in time graph.

Time of distances of vehicle distances covered with 6 mm hose for different pressures and weights are shown in Figure 12. It is seen that ideal times were provided with 50 kg weights for all three pressure. Similarly under 4 bars pressure, time increased with a rapid reaction at 100 kg weights. It was shown that 100 kg loads pressed the vehicle to the ground completely, and its wheels performed complete action. The ideal results for both experiments were obtained at 6 mm hose diameter, 4 bars pressure and 50 kg weight (Figure 11). Besides, 6 mm hose diameter provided an increase in efficiency in respect of distances compared to 8 mm hose diameter, 28% ($64 \cdot 100 / 50$) of lowest weight, and 37% ($50 \cdot 100 / 38$) at biggest weight. In these conditions, as theory muscular forces were calculated as 4158 (for three muscles), and the distances covered was found as 52 meters. Work done by the vehicle was obtained as 108108 Nm via work calculation formula. When considering ideal experimental conditions, which were 4 bars pressure

and 6 mm hose diameter and time 122 seconds, power of the vehicle was calculated as 886 Watt.

3. Conclusions

In this study, a movement mechanism running on pressurized air was developed with a pneumatic system, especially for light vehicle engines. The developed this prototype was tested by being assembled to an ATV having 110 cc engine capacities. With this study, minimization of energy consumption for movement of passenger cars, and using clean and cheap energy in vehicles were aimed. The produced mechanism can be an alternative among for single or two passenger vehicles in aspect of its small size compared to other vehicles in terms of zero pollution rates and low cost. In order to guide to forward studies with this subject, the obtained possible results are as follows:

- Pneumatic muscles used in a mechanism increased air consumption in big amounts, and they reduced the distance covered by designed vehicle. Accordingly, this situation also reduced efficiency of the vehicle.
- Cams are manufactured for every each valve appropriate to the muscle stroke, in order to provide synchronization of the muscles.
- In the result of the experiments, the maximum distance covered by the vehicle was 64 meters occurred at 50 kg weight, 4 bars pressure, 6 mm hose diameter and 143 seconds.
- When the distance covered by the mechanism with 6 and 8 mm hoses was

considered, average speed of vehicle was 0.45 m/sec.

- Under optimum conditions (hose 6 mm, pressure 6 bars and 150 kg weight) power of the vehicle was obtained as 886 Watt.

Application of energy sources as clean as electricity batteries that do not pollute the environment will provide a great decrease in carbon emission. New studies on the developed pneumatic movement mechanism will provide more efficiency to this developed mechanism. Especially, structural changes on movement transmission parts as crank shaft will increase efficiency of the mechanism. In this study, the designed cam system used in motion assembly is the best solution in such a mechanical movement system. In the later studies, programmable logic circuits (PLC) can be used in order to solve to possible synchronization problems of the pneumatic muscles. Another important factor in the study is capacity of the air tank. More air is needed for longer distances covered by vehicle. Therefore, this condition can be handled in later studies, particularly about development of tank capacity.

Funding

This project is supported by Gazi University Research Fund Project Number: 07/2012-52. The authors would like to thanks the Gazi University, Department of Scientific Research Projects, Ankara, Turkey, for financially supporting this research.

References

- [1] Verma, S. S. (2008). Air powered vehicles, *The Open Fuels&Energy Sci. J.* 1, 54-56.
- [2] Amaç A. &Şahin,C. (2009). Otomotiv güç sistemlerinin advisor tabanlı modellenmesi: geleneksel elektrikli ve hibrit elektrikli araçlar, 5. *Uluslararası İleri Teknolojiler Sempozyumu (IATS'09)*, Karabük.
- [3] Mistry,M.K.,Pravin P.R. &Sorathiya,A.S. (2012).Study and development of compressed air engine single cylinder: a review study, *International J. of Adv. Eng. Tech.* 3,1, 271-274.
- [4] Yadav,J. P. &Singh,B.R. (2011).Study and fabrication of compressed air engine, *Arabian Journal of Sci. Eng. And Tech.* 2, 2229-7111.
- [5] Patel,B.S.,Barot,M.R.,Shah, K.&Sharma P. (2011) Air powered engine, *Nat. Conf. on Recent Trends in Eng.&Tech.*, 1-4.
- [6] Thipse,S.S. Compressed air car, *Tech Monitor*, (2008) 33-37.
- [7] T. Sağır, (2006). Pnömatik motor tasarımı ve prototipinin imalatı, Yüksek Lisans Tezi, *Gazi Üniversitesi Fen Bilimleri Enstitüsü, Ankara*, 27-32.
- [8] Masood M., (2006). Compressed air engine: a new engine that can work on compressed air, *6th Saudi Technical Conference and Exhibition (STCEX6)*, Ryadh, 1-6.
- [9] Barycki,J. Ganczarek,M. Kollek,W. Mikulczynski, T. &Samsonowicz,Z. (2004). Performances of high-speed drive with self-acting impulse valve, *Mechanism and Machine Theory*, 39,6, 657-663.
- [10] Bozdemir,M.&Semiz,S. (2009) Levha kam mekanizmalarının bilgisayar yardımıyla tasarım ve imalatı, 5. *UluslararasıİleriTeknolojilerSempozyumu*, Karabük, 938-942.
- [11] Pekdur,Ö. Candan,C. Akdaş,D. &Akman, Y. (2012) Bilgisayarlı tasarım ve imalat yöntemleri kullanılarak krank mili imalatı, 3. *Ulusal Tasarım İmalat ve Analiz Kongresi, Balıkesir*, 568-573.
- [12] Şenol,R. Üçgül,İ.&Acar,(2006). M. Yakıt pili teknolojisindeki gelişmeler ve taşıtlara uygulanabilirliğinin incelenmesi, *Mühendis ve Makine* 47, 563, 37-50.
- [13] Khurmi, R.S. &Gupta,J.K. (2005). *A textbook of machine design*, Eurasia publishing
- [14] Wickramatunge,K.C.&Leephakpreeda,T. (2010). Study on mechanical behaviors of pneumatic artificial muscle, *Int. J. of Eng. Sci.* 48, 188-198.
- [15] Kerscher,T. Albiez,J. Zöllner,J.M. &Dillmann, R. (2006).Evaluation of the dynamic model of fluidic muscles using quick-release, in: *Proc.s of the First IEEE/RAS-EMBS Int. Conf. on Bio. Robotics and Biomechatronics Pisa*, 637-642.
- [16] Balasubramanian,K. &Rattan,K.S. (2005). Trajectory tracking control of a pneumatic muscle system using fuzzy logic, in: *Annual Conf. of the North American Fuzzy Infor. Proc. Society*, 472-477.
- [17] Leephakpreeda,T. (2012). Mathematical modeling of pneumatic artificial muscle actuation via hydrogen diving metal hydride-LaNi₅. *Journal of Bionic Eng.* 9, 110-118.
- [18] HuyAnhH.P.,Ahn, K.K. (2011). Hybrid control of a pneumatic artificial muscle (PAM) robot arm using an inverse NARX fuzzy model, *Eng. App. of Artificial Intel.* 24, 697-716.
- [19] Shi,G.L.&Shen W., (2013). Hybrid control of a parallel platform based on pneumatic artificial muscles combining sliding mode controller and adaptive fuzzy CMAC, *Control Eng. Practice* 21, 76-86.
- [20] Chandrapal,M. Chen,X. Wang,W. &Hann,C. (2012) Nonparametric control algorithms for a pneumatic artificial muscle, *Expert Systems with App.* 39, 8636-8644.
- [21] Andrikopoulos,G. Nikolakopoulos,G. &Manesis S., (2013). Pneumatic artificial muscles: A switching model predictive control approach. *Control Eng. Practice* 21,12, 1653-1664.
- [22] Ganguly,S. Garg,A. Pasricha,A. &Dwivedy,S.K. (2012) Control of pneumatic artificial muscle system through experimental modelling, *Mechatronics*, 22, 8, 1135-1147.
- [23] Yılmaz,M. Karakaş,E. Çolak,Z. G. &Kuzucu,A. (2008) Pnömatik yapay kaslı robot kolunun konum kontrolü, *Mühendis ve Makine*, 50, 589: 13-23.

- [24] Chivu,C. (2007). Static model and simulation of a pneumatic artificial muscle. *Int. Conference on Economic Eng. and Manufac. Systems*, 8,3a(21a), 239-242.
- [25] DaerdenF. F. (1999). Conception and realization of pleated pneumatic artificial muscles and their use as compliant actuation elements. *Phd. Dissertation, University of VrijeBrussel*.
- [26] Klute,G. K. Czerniecki,J.M. &Hannaford, B. (1999). McKibben Artificial muscles: Pneumatic actuators with biomechanical intelligence. *Int. Conference on Adv. Intelligent Mechatronics (AIM '99)*, Atlanta, September, 19-22.
- [27] Ferrari,Z.G. Lucio,C. Giovani,G. Ignacio S. M., &Andre,P.E. (2010). Static modelling of mckibben pneumatic muscle, *ABCM Symposium Series in Mechatronics*, 4, 914-922.
- [28] Yeh, T-J. Je Wu, M. Lu,T-J. Wu,F-K.&Huang, C-R. (2010) Control of McKibben pneumatic muscles for a power-assist, lower-limb orthosis. *Mechatronics*, 20, 686–697.
- [29] Kenneth,K.K. &Bradbeer,R. Static model of the shadow muscle under pneumatic testing, *Depart. of Electric Eng.*, City University of Hong Kong. Project number: U 1146/04E.
- [30] Thompson, F. &Haywood, G. G. (1986). Structural analysis using virtual work. *SponPress*, 1-4.

Corresponding author: Gürcan Samtaş

Institution: Düzce University Engineering Faculty,
Department of Mechatronics, Beci, Düzce,
Türkiye

E-mail: grcann@gmail.com